Mathematical Model for Dynamics of CSF through the Aqueduct of Sylvia Based on an Analogy of Arterial Dilation and Contraction

Amila Thalakotunage[1] and Thunyaseth Sethaput[2]

***Abstract*-**Hemodynamics studies of cerebral blood and governing of cerebrospinal fluid (CSF) are important circumstances for diagnosis of many diseases associated with human brain like hydrocephalus, brain trauma and increased intracranial pressure (ICP). CSF is genesis by epithelial cells of choroid plexuses in ventricles and secretes to subarachnoid spaces (SAS) and lumbar CSF spaces through the cerebral aqueduct. Non-invasive methods on computational analysis and mathematical models to predict dynamic behavior and CSF motion are yet to be developed. This study is extended to develop a mathematical model to predict CSF motion through the cerebral aqueduct based on an arterial compliance. Throughout of our study, region of interest (ROI) was the cerebral aqueduct and considered both blood vessel and aqueduct walls as linear spring system of two degree of freedom. Results of math model showed, contraction and dilation of arteries contributes significant role for governing force of CSF by inheriting pulsatile motion, which synchronized with pulsatile motion of blood, but with having a phase shift with a blood motion.

***Keywords*-**Cerebrospinal fluid, cerebral aqueduct, Arterioles dilation, Math model.

I. INTRODUCTION

CEREBROSPINAL fluid (CSF) is a colourless fluid contained of blood plasma and permeates through the subarachnoid spaces by surrounding brain [1]. Formation of CSF is befall of four cavities in brain called ventricles and circulates through the ventricular system. This layer of liquid in ventricular system delivering nutrients to brain, remove the waste products from cellular metabolism and protects the human brain from shocks by acting as shock absorber [2]. Under the normal physiological condition, CSF maintains a pulsatile flow of motion due to systolic expansion and constriction of the intracranial arteries causing constriction and dilation of ventricles simultaneously. During the systole and diastole, CSF shows antagonistic pulsatile motion with respect to cardiovascular pulsation and flows in bulk with each cardiac cycle [3]. Greitz D [3] has shown, flow sensitive MRI authenticate that bulk flow of CSF excreted in cerebral aqueduct.

[1, 2]Manufacturing Systems and Mechanical Engineering (MSME) Department

Sirindhorn International Institute of Technology, Thammasat University, Thailand

Monro-Kellie hypothesis states that, skull is enclosed container consistence with brain (80%), intracranial blood (10%), cerebrospinal fluid (10%), and sum of the volumes of these three components are constant. Increment or decrement of volume in either one of these contents must be compensate by reducing or increasing in volume of other contents. CSF and intracranial blood can easily adapt to compensate the volume changes. If this compensatory mechanism is exhausted, further change of volume of one content can leads to rise or decrees of intracranial pressure (ICP) [5]. Overproduction or inadequate re-absorption of CSF and disorders in CSF pathway (cerebral aqueduct) will result in over accumulation of cerebrospinal fluid in ventricles result in enlargement of brain and can be the cause of disease in ICP and hydrocephalus. Under these circumstances, better understanding of CSF dynamic, regulation of cerebral blood flow (CBF) and its waveform are helpful for the prognosis of diseases associated with cerebrospinal fluid.

In 1978, A. Marmarou et al [6] bring forwarded an important hypothesis for kinetic of the intracranial pressure. The time course was measured based on four parameters; intracranial compliance, dural sinus pressure, resistant to absorb CSF and cerebrospinal formation and role of each parameter to governing the dynamic equilibrium of ICP was measured. In his mathematical model; newly formed CSF (I_f) subdivided to two components; CSF retained within the SAS (I_s) and amount of CSF absorbs to venous blood arteries (I_a). Controversial circumstance of this model is they considered as CSF pressure are maintained at constant pressure. Since CSF has pulsatile nature of dynamic behaviour, constant pressure cannot be account.

Periodically, several researchers have been interpreted mathematical models for the CSF dynamics based on experimental and clinical-pathological observations. Hakim et al [7] suggest some classical concepts of physics to explain about the rational mechanics of the cranial content and shown that, how the intraventricular pressure gradient creates stress on brain parenchyma and its variation throughout the CSF production.

Mauro Ursino [8], [9] has proceeded an A mathematical study of human intracranial hydrodynamics based on the cerebrospinal fluid pulse pressure and auto regulation. But his studied despite to consider the influence of cardiac cycle in term of the pulsatile motion of cerebrospinal fluid.

However, recently Simone Bottan et al. [10] formed a 3D Phantom model of cranial system and analysed the

physiologic cerebrospinal fluid dynamics by considering bulk and pulsatile physiologic CSF flow. Similarly, Ambarki et al [11] developed an A new lumped-parameter model of CSF hydrodynamics throughout the cardiac cycle in healthy volunteers and was able to analyse the time domain characteristics including time shift of arterial and CSF flow.

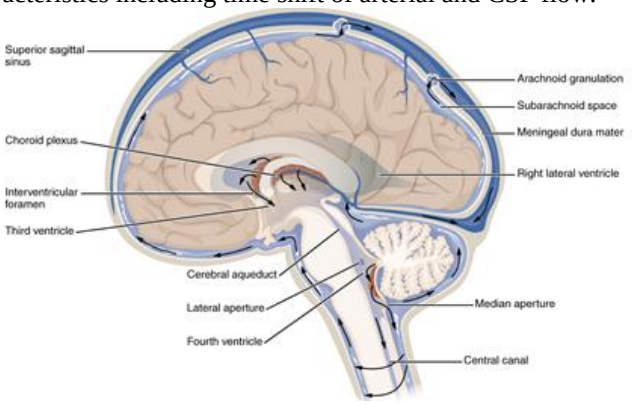

Fig. 1: CSF Pathway in Human Brain [15]

Fig. 1 shows the pathway of CSF. Cerebrospinal fluids primarily generating in four sites names in consecutively, Lateral ventricles, third ventricles and fourth ventricles. CSF formatted in lateral ventricles enters to the third ventricles through the Intraventricular foramen and third ventricles to fourth ventricles via the cerebral aqueduct.

In the contest of CSF pulsatile motion analysis, the hypothesis of Linninger et al. [12] plays a vital role. Their model of fluid structure interactions was able to predict the flows and pressures patterns throughout the brain's ventricular pathways and quantifies the pulsatile CSF motion including flow reversal in the cerebral aqueduct.

In this context, we developed a mathematical model to imply the pulsatile motion of CSF through the cranial space based on the analogy of arterial dilation and contraction. Main advantage of this method is been a non-invasive method. Monitoring and cognizance of parameters of CSF like, flow pattern, periodicity and flow rate -helps physicians to systematically analyse and diagnosed the disorders associated with intracranial hydrodynamic of any patient by comparing with normal physiological condition.

II. METHODOLOGY

In this comprehensive study, we paid our attention for deeper insight of dilation and contraction of blood vessels, mechanical forces exerted on the blood vessel inner wall while using basic principles of fluid mechanics and theory of spring damper analysis. Conclusively emphasis, CSF pulsatile motion is dominantly driven by dilation and contraction of arteries due to its pulsatile motion of blood. The source of our study was the former retrospective study of "Pulsatile Cerebrospinal Fluid Dynamics in the Human Brain" by Andreas A. Linninger et al.[12-13]. Their model was adequate to quantify the pulsatile volumetric flow motion of CSF through the cerebral aqueduct.

Flow sensitive MRI investigations has shown, CSF flows as bulk in each cardiac cycle and most prompt CSF bulk flow occurred in our ROI [3-4]. The bulk flow velocity of CSF deduct to the ratio of 3:1 by aqueduct in order to maintain continuous flow to the site of cranium space [14]. These results was increased our curiosity to make a math model for understand the physiological phenomenon of cerebral aqueduct by selecting as region of interest. Clear understanding on phenomena of CSF driving force and its flow pattern helps physicians to discriminate abnormalities with the normal physiological conditions.

2.1 Arterial Compliance

Active Transportation Of Blood In Human Beings Is Primarily Governed By The Cardiac Cycle. The Blood Circulatory System Is A Closed Organon And Transport Blood From The Heart To Capillaries And Capillaries To Heart In Unidirectional Way. Arterial Vessels Are Not Totally Rigid And Its Elastic Nature Conduced Forth And Continuous Motion Of Blood By Disrupting The Reverse Motion. Oscillatory Movements of Blood Flow Enlarge the Elastic Artery Resultant of Systolic Flow Induced Pressure and Facilitate an Accommodation for Additional Blood Volume. Diastolic Recoil Of Arterial Wall Thrust The Additional Blood Volume And Maintains Continuous Blood Flow To The Forth During Systole And Diastole. The Mechanism Is Also Known As The Windkessel Effect Which Has Introduced By Otto Frank [16]. Relationship Between Volumetric Changes Of Arterial Blood (ΔV) Due To The Particular Arterial Blood Pressure Change (ΔP) Can Be Quantified As Compliance (C) [17].

$$C = \Delta V / \Delta P \tag{1}$$

For Assessments, Cross-Sectional Compliance (CC) Is Considered Due To The Inappreciable Amount Of Strain Along The Longitudinal Direction Of Blood Vessel And Volumetric Change Is Evaluated In Radial Direction. Cross-Sectional Compliance Interprets As The Ratio Of Arterial Cross-Sectional Area (ΔA) To Pressure Difference (ΔP) [18].

$$CC = \Delta A / \Delta P \tag{2}$$

Arterioles Are Form With Endothelium And Vascular Smooth Muscles. These Two Layers Exhibit Stiff and Springy Properties by Elastin Vessel to Sustain In Higher Pressure. Vascular Smooth Muscles Respond Even For A Small Pressure Drop By Stretching The Diameter And, Change Of Diameter Can Dramatically Influenced To The Adjustment Of Arterial Blood Flow Resistant. By Assuming That Blood Flow Is Steady and Vessel Is Rigid and Uniform, Resistant of Blood Flow Can Be Computed Using Hagen Poiseuille's Rational.

$$R_{Arterial} = 8\eta L / \pi r^4 \tag{3}$$

{Where; *H* Is Blood Viscosity, *L*-Length of Blood Vessel and *R* Is Radius.}

Arterial Compliance Balance the Pressure Gradient Corresponds To the Variation of $R_{arterioles}$. Under The Normal Physiological Condition of Young Healthy Person, Pulsatile Blood Pressure Fluctuates Between 80 mmhg Diastolic and 120 mmhg of Systolic Pressure. To The Mathematical Applications, Mean Arterial Pressure (MAP) Is Considered As the Average Driving Pressure And Can Be Calculated As,

$$MAP = P_{Diastolic} + (1/3)\left(P_{Systolic} - P_{Diastolic}\right) \tag{4}$$

2.2 Former Model By Linninger Et.Al

The Model Proposed By Linninger Et.Al [12] Followed The First Principles Of Fluid Dynamics In Order To Calculate CSF Pressure And Velocity Variation Over The Brain. They Treated As; Kinetic Energy Of Arterial Compression On The Choroid Plexus Is Basically Affected To The Pulsatile Motion Of CSF Dynamic And Brain Parenchyma Gives A Feedback To Its Auto-Regulation. To Simplify The Complexity Of Mathematical Application, One Dimensional Framework Has Used. Navier-Stocks And Momentum Equation Were Used To Acquire The Fluid Dynamics Results And Some Of Elastostatic Laws Were Used To Compute Stresses And Strains On Brain Parenchyma. Fig. 2 Shows The Model Which Is Illustrating Of Ventricles And Its Displacement Due To The Forces Act On Elastic Brain Tissues.

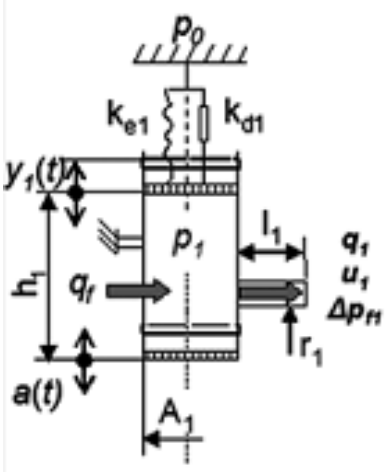

Fig. 2: Forces Imparted On Ventricles And Its Displacement [12]- Edited. Linear Elastic Springs Represent The Periventricular Tissues.

To quantify the parenchymal tissue deformation, the standard thin elastic membrane model of Brooks et.al [19] were applied by only considering epithelial layer in the peri-ventricular area. The pressure difference between CSF pressure in ventricles (p_i) and pressure of brain parenchyma (p_o) caused to the expansion of ventricular wall. The acceleration of membrane element showing in Fig. 2 employed by three forces; pressure difference of CSF and brain tissues (p_i-p_o), epithelial tissue elasticity ($k_e.y_i$) and dissipative force ($k_d.\dot{y}_i$). Inside of ventricles are filled with cerebrospinal fluid and compressed the walls due to the inbuilt pressure. Oscillatory motion of choroid expansion and contraction synchronized with the cardiac cycle and presented as the force function;

$$a(t)=\alpha\left(1.3+\sin\left(\omega t-(\pi/2)-0.5\cos\left(2\omega t-(\pi/2)\right)\right)\right) \quad (5)$$

Important fact is, foramen of monro was considered as an elastic tube. Moreover, average axial velocity (v_i) has counted for the moment balance and radial moment balance were neglected. The rate of change in tissue deformation ($\dot{y}_i$) is equate to the radial velocity and volumetric change has quantified by $A.\dot{y}_i(t)$. According to the basic principles of the hydrodynamics, fluid flows from region of high pressure to region of low pressure. In fact, CSF flows from ventricles to veins where it is absorbed. Kinetic of CSF is betiding as a result of pressure drop among the SAS and arachnoid villi.

By applying newton's second law of motion for the equilibrium condition of motion under the three forces; force exerted on the ventricular wall due to the pressure difference (P_i-P_o), elastic tissue compliance ($k_e.y_i(t)$) and dissipation by first order damping force ($k_d.\dot{y}_i(t)$). Acceleration of brain parenchymal tissues was derived as in (6).

$$(\rho_\omega A_i\delta)\ddot{y}_i(t)+k_d\dot{y}_i(t)+k_e y_i(t)-A_i\left[p_i(t)-p_o(t)\right]=0 \quad (6)$$

$$i\in\{LV_1-LV_4, SAS\}.$$

Continuity of cerebrospinal fluid throughout the ventricles was derived as;

$$\partial\left\{A_i\left[h_i+a(t)+\dot{y}_i(t)\right]\right\}/\partial t=q_{f,i}-q_i, \quad i\in\{LV_1-LV_4\} \quad (7)$$

Axial moment upon the foramen of monro,

$$\rho\left[(\partial v_i/\partial t)+v_i(\partial v_i/\partial z)\right]+\partial p_i(t)/\partial z=-F_i, \quad i\in\{FM, AS, FL\} \quad (8)$$

Where, $F_i=(8\mu/r_i^2)v_i$

All the equations were solved in Laplace domain by the Simulink MATLAB platform and characteristic mechanical properties of CSF and tissues used to compute the equations are tabulated in TABLE I.

TABLE I
CHARACTERISTIC MECHANICAL PROPERTIES OF CSF AND TISSUES

Property	Value
Young Modulus for ventricles	2,100 N/m^2
Young Modulus for SAS	3,500 N/m^2
CSF density, ρ_f	1,004-1,007 kg/m^3
Density of blood , ρ_B	1025 kg/m^3
CSF Viscosity, μ_{CSF}	10^{-3} Pas
Ventricular tissue Spring elasticity, k_e	8 N/m (Normal)
Brain tissue Dampening , k_d	0.35×10^{-3} (Ns)/m
Spring elasticity of Arterioles , k_B	10 N/m (Assume)
Ependyma density , ρ_ω	1,000 kg/m^3
Reabsorption constant, k	1.067×10^{-11} m^3/(Pas)

After computing the math model, they have seen maximum velocity occurred through the aqueduct of Sylvia as +25.8 mm/s and -21.7 mm/s. Nevertheless, literature values of CSF velocity via the aqueduct of Sylvia based on the clinical observations shows a deviation from this value [20],[21],[22],[23].

Despite the fact that many hypothesis have exhibited, non-of explain how mechanical energy of blood pulsatile motion transmit to the CSF motion. Since, blood circulatory system is fully enclosed circuit, there might not be any fluid interaction between cerebral blood and CSF accept in the venous blood at arachnoid villi.

2.3 Transmit Of Mechanical Energy From Arteries To CSF

In this hypothesis, we bring forward that CSF pulsation dominantly occurs due to the pulsatile movement of blood. Mechanical energy dissipates during the dilation and contraction of blood vessel transmits to ventricular system in order to generate oscillatory motion of CSF. Arteriole wall

and ventricular tissues were substitute in to two elastic springs and connected each in series. Few assumptions have made as; springs are frictionless, massless, springs are obeying with Hooke's law and consider only in linear elastic range. Fig. 3 shows the model of arteriole and ventricular springs, forces exerted on arteriole inner wall and its dilation.

$$Q_{in} = Q_{Stored} + Q_{Out} \quad (9)$$

Force applies on arteriole inner wall (FB) is equal to MAP time projected area of inner wall.

$$F_B = MAP \times A_B \quad (10)$$

$$F_B = \left\{ P_{Diastolic} + (1/3)\left(P_{Systolic} - P_{Diastolic} \right) \right\} \times r_B \times l_B \quad (11)$$

For an equilibrium condition of spring system can be mathematically model as;

$$m_B \delta\ddot{r} = F_B(t) + k_B\left(y_i(t) - \delta r \right) \quad (12)$$

Newton's second law of motion has been applied to the blood element and m_B is the mass of blood element. Under the equilibrium state, m_B time acceleration of radial displacement equals to the sum of force applies on the arteriole inner wall and resultant spring force of arteriole with respect to relative displacement of arteriole and ventricular tissues.

$$m_{CSF}\ddot{y}_i(t) = -k_B\left(y_i(t) - \delta r \right) - k_e y_i(t) \quad (13)$$

By applying Newton's second law for the ventricular tissue spring, equilibrium can be stated as in (13).

For system balance, two equations can be written in matrix form,

$$\begin{pmatrix} m_B & 0 \\ 0 & m_{CSF} \end{pmatrix}\begin{pmatrix} \delta\ddot{r} \\ \ddot{y}_i \end{pmatrix} + \begin{pmatrix} k_B & -k_B \\ -k_B & (k_B + k_e) \end{pmatrix}\begin{pmatrix} \delta r \\ y_i \end{pmatrix} = \begin{pmatrix} F_B(t) \\ 0 \end{pmatrix}$$

MATLAB® Simulink has been used as mathematical platform to plot the displacement of ventricular tissues with respect to the displacement of arteriole wall. Unit impulse input was applied. Quantitative values for each parameter are showing in TABLE I and elastic constant for an arteriole has assumed as 10 N/m.

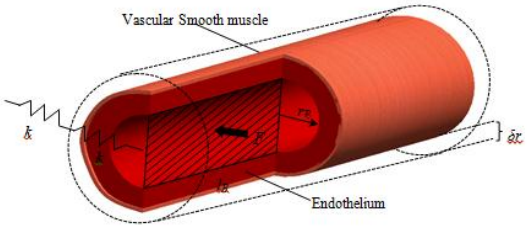

Fig. 3: Model of Arteriole and Ventricular Springs

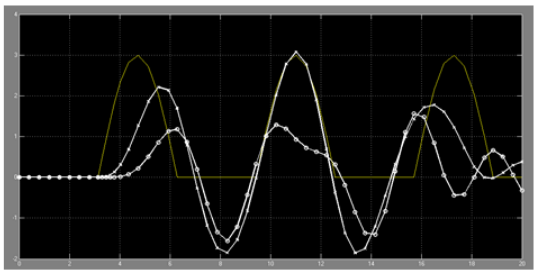

Fig. 4 Displacement of Artery Wall and Ventricular Tissues under the Pulsatile Input. Vertical Axis Denotes the Millimetre and Horizontal Axis Denotes R-R Cardiac Intervals

According to the Simulink simulation results, displacement of artery wall and ventricular tissues shows a pulsatile variation as in fig. 4. $\delta r(t)$ and $y_i(t)$ represent the blood wall displacement and ventricular tissue displacement correspondingly. To simulate the model in realistic manner, impulse signal has been given to the springs as input since cardiac pulse almost similar to impulse signal.

Isomorphism of cardiac pulse wave and ventricular tissue displacement during the one single cardiac cycle benefits to validate our model, which demonstrates the correlation of blood vessel dilation and ventricular displacement in the aspect of two springs which connected in series. In addition, similarity of aqueductal CSF flow corroborates the correlation between ventricular tissue displacement and cardiac pulsatile motion. Moreover, to confirm the relevance of ventricular tissue displacement and CSF velocity through the aqueduct, we defined a simple model for the CSF trapped in ventricular cavity. For a normal healthy person, ventricular cavity accommodates 25-30 ml of CSF in one time. In this approach we liken ventricular cavity as a sphere with one degree of freedom to deform and considered the volume of CSF in ventricle at one time as 27.5 ml. Radius of model sphere (r_{Sphere}) for 27.5 ml volume is 18.72 mm. Since ventricular cavity is enclosed volume, same -amount of CSF with respect to the volumetric displacement due to the y_i should leave from the site. Aqueduct of Sylvia acts as the passage way to escape the displaced volume of CSF. According to the cine phase MRI studies [26], cross sectional area of aqueduct ($A_{aqueduct}$) has given as 3 cm^2. By examine relevant parameters, velocity of CSF through the aqueduct ($V_{CSF\ aqueduct}$) for a normal subject can be mathematically modelled as;

$$A_{aqueduct} \times V_{CSF\ aqueduct} = (4\pi/3)\left\{ r_{Sphere}{}^3 - \left(r_{Sphere} - y_i \right)^3 \right\} \quad (14)$$

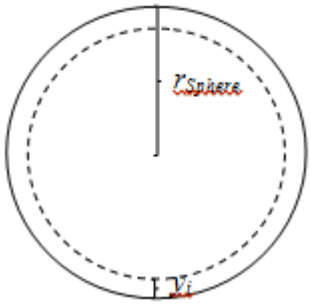

Fig. 5: Ventricular cavity assigned as sphere.

III. Results and Discussions

Based on the reciprocate movement of y_i and clinical measurements of CSF velocity variation pattern; we stated that, variation of ventricular volume change is proportional to the y_i. Acquired volume of ventricles due to the displacement of tissues, increase the pressure inside ventricles. To compensate the volume change, CSF in the ventricles has to be removed from ventricular space. By applying maximum ventricular tissue displacement (y_i) in to the (14), maximum velocity of CSF through the aqueduct can be calculated as

2.275 cm/sec for 1.7mm of y_i and $A_{Aqueduct}$= 3cm^2. To validate the results of math model and its correlation with Simulink results, we used real CSF velocity data's of ten healthy subjects which measured by Haughton VM et all [23]. Their results show in TABLE II, the average peak systolic velocity is 2.36 cm/s. With that validation, peak systolic CSF velocity can be written as 2.2±0.2 cm/s.

TABLE II
CSF VELOCITY VALUES FOR TEN HEALTHY SUBJECTS-[23]

Volunteer No:	Age (years)	Peak Systolic velocity (cm/s)	Peak Diastolic velocity (cm/s)
1	61	2.1	2.4
2	36	1.7	2.1
3	28	2.0	1.6
4	21	2.7	4.2
5	33	2.9	1.9
6	48	1.2	2.1
7	41	2.2	4.5
8	47	2.4	2.5
9	46	3.3	3.5
10	30	3.1	2.9
Average	39.1	2.36	2.77

According to the simulation results of our model; CSF velocity pattern through the aqueduct and its correlation with ventricular tissue displacement are shown in fig. 6. Results shows, CSF flow velocity proportional to the ventricular displacement and CSF flow is synchronized with cardiac pulsation with making a small phase shift.

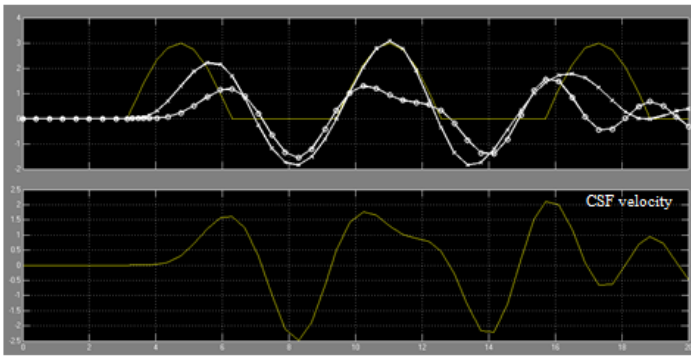

Fig. 6: CSF Velocity Profile through the Aqueduct With Respect To Ventricular Tissue Displacement. CSF Velocity In Terms Of "Cm/Sec" In Term of Cardiac R-R Intervals

Giovanni de Marco et al.[22] have measured net aqueductal CSF flow velocities of normal subject in three times over ten month period by using phase-contrast cine MR imaging. Aqueductal CSF velocities profiles of their clinical observation are showing in fig. 7, and velocity variation is similar with our simulation results during one cardiac cycle.

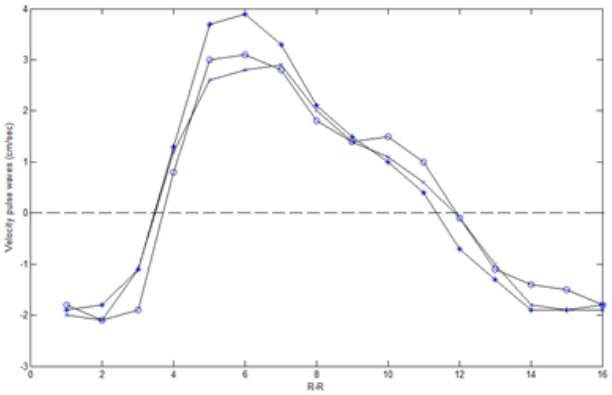

Fig. 7: Aqueductal CSF Flow Velocities Of Normal Subject In Three Times Over Ten Month Period [22]-Edited.

R-R interval denotes the time interval between two corresponding ventricular depolarization. Velocities above the horizontal axis represent the CSF flow in the craniocaudal direction and below the horizontal line represent caudocranial direction of flow [24].

IV. CONCLUSION

By comparing actual clinical data of peak systolic and peak diastolic velocity of CSF and simulation results, we can conclude that governing force of CSF motion is dominantly governed by arterial wall expansion and contraction in radial direction. CSF motion is synchronized with cardiac pulsation and shows reciprocate motion. An extensive studies of CSF dynamic behaviours helps to diagnose many diseases like Hydrocephalus, Cerebral edema, malignant infarction and subarachnoid haemorrhage etc. This math model can be used to model the CSF dynamic motion based on cardiac pulsation and further studies will leads to find diagnosis methods for particular diseases.

V. NOMENCLATURE

A_i	Cross section of the ventricular or sub-arachnoid section [m^2]
A_B	Projected cross section area of Arterioles inner wall [m^2]
$a(t)$	Choroid plexus displacement [m]
h_i	Height of the ventricular or subarachnoid section [m]
k_e	Brain tissue elasticity constant [N/m]
k_d	Brain tissue compliance [(N s)/m]
k_B	Spring constant of Arterioles [N/m]
F_i	Poiseuille Friction term [N/m^3]
F_B	Force exerted on internal wall of Arterioles [N]
l_i	Length of foramina connecting ventricles [m]
l_B	Length of Arterioles blood vessel [m]
$p_o(t)$	Pressure of brain parenchyma [N/m^2]
$p_i(t)$,$p_{SAS}(t)$	CSF pressure in ventricles and subarachnoid section (ICP) [N/m^2]
$q_{e,i}(t)$	Reabsorption flow rate in a section [m^3/s]
$q_{f,i}(t)$	CSF production rate in the choroid plexus [m^3/s]
$q_i(t)=A_i\upsilon$	CSF flow rate leaving ventricle, i.e., flow in

$_i$	foramina and aqueduct [m^3/s]
r_i	Radius of the foramina and aqueduct [m]
r_B	Internal radius of Arterioles vessel [m]
$v_i(t)$	Axial CSF flow velocity [m/s]
$y_i(t)$	Tissue displacement in a section [mm]
$P_{Systolic}$	Systolic blood pressure [N/m^2]
$P_{Diastolic}$	Diastolic blood pressure [N/m^2]
Greek Symbols	
δ_r	Arterioles wall displacement [m]
α	Amplitude of choroid expansion [m]
δ	Tissue width [m]
k	Reabsorption constant [$m^3/(Pa\ s)$]
μ	Fluid density [kg/m^3]

VI. References

[1] Nafiseh Masoumi, Dariush Bastani, Siamak Najarian, Fariba Ganji, Farhad Farmanzad, and Amir Saeed Seddighi. "Mathematical Modeling of CSF Pulsatile Hydrodynamics Based on Fluid–Solid Interaction". IEEE TRANSACTIONS ON BIOMEDICAL ENGINEERING, VOL. 57, NO. 6, JUNE 2010

[2] Overview of Adult Intracranial Pressure (ICP) Management & Monitoring Systems, Orlando Regional Healthcare, Education & Development ©Copyright 2003.

[3] Greitz D, "Cerebrospinal fluid circulation and associated intracranial dynamics. A radiologic investigation using MR imaging and radionuclide cisternography," Acta Radiologica. Supplementum [1993, 386:1-23]

[4] Michael Egnor, Lili Zheng, Arthur Rosiello, Fred Gutman and Raphael Davis, "A Model of Pulsations in Communicating Hydrocephalus," Pediatric neurosurgery

[5] Laurence T Dunn, "RAISED INTRACRANIAL PRESSURE," J Neurol Neurosurg Psychiatry 2002;73:i23-i27

[6] Anthony Marmarou, Ph.D, Kenneth Shulman, M.D, and Roberto M. Rosende, M.D, "A Nonlinear analysis of the cerebrospinal fluid system and intracranial pressure dynamics," J Neurosurg 48:332-344, 1978

[7] Hakim S, Venegas JG, Burton JD, "The physics of the cranial cavity, hydrocephalus and normal pressure hydrocephalus: mechanical interpretation and mathematical model," Surg Neurol. 1976 Mar; 5(3):187-210. PubMed PMID: 1257894

[8] Mauro Ursino, "A mathematical study of human intracranial hydrodynamics part 1—The cerebrospinal fluid pulse pressure," Annals of Biomedical Engineering. Vol. 16, pp. 379-401. 1988

[9] Mauro Ursino, "A mathematical study of human intracranial hydrodynamics part 2—Simulation of clinical tests," Annals of Biomedical Engineering. Vol. 16. pp. 403-416. 1988

[10] Simone Bottan, Dimos Poulikakos, and Vartan Kurtcuoglu, "Phantom Model of Physiologic Intracranial Pressure and Cerebrospinal Fluid Dynamics," IEEE TRANSACTIONS ON BIOMEDICAL ENGINEERING, VOL. 59, NO. 6, JUNE 2012

[11] Ambarki, K. and Baledent, O. and Kongolo, G. and Bouzerar, R. and Fall, S. and Meyer, "A New Lumped-Parameter Model of Cerebrospinal Hydrodynamics During the Cardiac Cycle in Healthy Volunteers," *IEEE Transaction on Biomedical Engineering*, Vol. 54. pp. 483-491. 2007

[12] Andreas A. Linninger, Cristian Tsakiris, David C. Zhu, Michalis Xenos, Peter Roycewicz, Zachary Danziger, and Richard Penn, "Pulsatile Cerebrospinal Fluid Dynamics in the Human Brain" . *IEEE TRANSACTIONS ON BIOMEDICAL ENGINEERING*, VOL. 52, NO. 4, APRIL 2005

[13] Andreas A. Linninger, Michalis Xenos, David C. Zhu, MahadevaBharath R. Somayaji, Srinivasa Kondapalli, and Richard D. Penn., "Cerebrospinal Fluid Flow in the Normal and Hydrocephalic Human Brain," *IEEE TRANSACTIONS ON BIOMEDICAL ENGINEERING*, VOL. 54, NO. 2, FEBRUARY 2007

[14] Naidich TP, Altman NR, Gonzalez-Arias SM, "Phase contrast cine magnetic resonance imaging: normal cerebrospinal fluid oscillation and applications to hydrocephalus," Neurosurg Clin N Am. 1993 Oct;4(4) 677-705

[15] http://en.wikipedia.org/wiki/Cerebrospinal_fluid#/media/File:1317_CFS_Circulation.jpg

[16] O. Frank, "Die grundform des arteriellen pulses. Erste Abhandlung, Mathematische analyse," Z. Biol., vol. 37, pp. 483-526, 1899

[17] Spencer, M.P and Dennison, A.B, "Pulsatile blood flow in the vascular system. In "Handbook of Physiology," Vol.2, Sect.2, pp.839-864, American Physiology Society, Washington, D.C. (1963)

[18] Robert S. Reneman, Tiny Van Merode, Paul Hick, Arno M.M. Muytjens, Arnold P.G. Hoeks, "Age-related changes in carotid artery wall properties in men," Ultrasound in Medicine & Biology. Volume 12, Issue 6, June 1986, Pages 465–471

[19] Brook, B.S., Falle, S.A.E.G. and Pedley, T.J, "Numerical solutions for unsteady gravity-driven flows in collapsible tubes: evolution and roll-wave instability of a steady state," Journal of Fluid Mechanics, 396. pp. 223-256 (1999)

[20] Naidich TP, Altman NR, Gonzalez-Arias SM, "Phase contrast cine magnetic resonance imaging: normal cerebrospinal fluid oscillation and applications to hydrocephalus" Neurosurg Clin N Am. 1993 Oct;4(4) 677-705

[21] Dieter R. Enzmann and Norbert J. Pelc, "Cerebrospinal Fluid Flow Measured by Phase-Contrast Cine MR," AJNR 14:1301-1307, Nov/ Dec 1993

[22] Giovanni de Marco, Ilana Idy-Peretti, Anne Didon-Poncelet, Olivier Baledent, Fannie Onen and Marie Ce´cile Henry Feugeas, "Intracranial Fluid Dynamics in Normal and Hydrocephalic States Systems Analysis With Phase-Contrast Magnetic Resonance Imaging," J Comput Assist Tomogr. Volume 28, Number 2, March/April 2004. NEUROIMAGING

[23] Victor M. Haughton, Frank R. Korosec, Joshua E. Medow, Maria T. Dolar, and Bermans J. Iskandar, "Peak Systolic and Diastolic CSF Velocity in the Foramen Magnum in Adult Patients with Chiari I Malformations and in Normal Control Participants," AJNR Am J Neuroradiol 24:169–176, February 2003

[24] Hueng-Chuen Fan, Lung-Hui Giiang, Teng-Yi Huang, Chun-Jung Juan, Cheng-Yu Chen, Ann-Chin Wang and Shyi-Jou Chen, "Cerebrospinal Fluid Flow Quantification of the Cerebral Aqueduct in Children and Adults with Two-Dimensional Cine Phase-Contrast Magnetic Resonance Imaging," Fu-Jen Journal of Medicine Vol.9 No.2 2011